HHS Public Access

Author manuscript

Nat Immunol. Author manuscript; available in PMC 2016 November 02.

Published in final edited form as:

Nat Immunol. 2016 July ; 17(7): 825–833. doi:10.1038/ni.3463.

A TRAF-like motif of ICOS controls development of germinal center T follicular helper cells via TBK1

Christophe Pedros[1], **Yaoyang Zhang**[2], **Joyce K. Hu**[3], **Youn Soo Choi**[3,5], **Ann J Canonigo-Balancio**[1], **John R. Yates III**[2], **Amnon Altman**[1,‡], **Shane Crotty**[3,4,‡], and **Kok-Fai Kong**[1,‡]

[1]Division of Cell Biology La Jolla Institute for Allergy and Immunology, La Jolla, California

[2]Department of Chemical Physiology, The Scripps Research Institute, La Jolla, California

[3]Division of Vaccine Discovery, La Jolla Institute for Allergy and Immunology, La Jolla, California

[4]Division of Infectious Diseases, School of Medicine, University of California San Diego, La Jolla, California

Abstract

Inducible costimulator (ICOS) signaling fuels the stepwise development of T follicular helper (T_{FH}) cells. However, a signaling pathway unique to ICOS has not been identified. We show that TANK-binding kinase 1 (TBK1) associates with ICOS via a conserved motif, IProx, which shares homology with tumor necrosis factor receptor (TNFR)-associated factors, TRAF2 and TRAF3. Disruption of this motif abolishes the association with TBK1, thus identifying a TBK1-binding consensus. Mutation of this motif in ICOS, or depletion of TBK1 in T cells severely impaired the differentiation of germinal center (GC) T_{FH}, B cell and antibody responses, but was dispensable for early T_{FH} differentiation. These results reveal a novel ICOS-TBK1 signaling pathway that specifies GC T_{FH} cell commitment.

Diversification of antigen receptors in higher organisms is an evolutionary adaptation to the rapid mutability of the ever-evolving microorganisms. The ability to generate high-affinity neutralizing antibodies (Abs) protects the host from invading pathogens. Nonetheless, the process of diversifying antigen receptors intrinsically carries the risk of self-antigen recognition, leading to destruction of self-tissues and autoimmune manifestations. One of the safeguard mechanisms is to insulate the Ab-generating machinery to a specialized anatomical compartment, known as the germinal center (GC), embedded within secondary

Correspondence should be addressed to: Kok-Fai Kong (kfkong@lji.org) and Shane Crotty (shane@lji.org).

‡These authors share senior authorship.

[5]Current Address: Transplantation Research Institute, Department of Medicine, Seoul National University College of Medicine, Seoul, South Korea.

Author Contributions: C.P. and A.J.C. designed experiments, collected data, and performed analyses; Y.Z. and J.Y. did the proteomic experiment and analyses; J.H. did the immunofluorescence and microscopy; Y.S.C. provided critical reagents and were involved in study design; A.A., S.C. and K.F.K. designed the study, analyzed data and wrote the paper.

Competing Financial Interest: The authors declare no competing financial interests.

Author Information Reprints and permission information is available at www.nature.com/reprints. Readers are welcome to comment on the online version of the paper.

lymphoid organs. Inside GCs, B cells undergo successive rounds of random somatic hypermutation, affinity maturation and isotype class switching[1]. Only B cells expressing high-affinity, class-switched Abs specific for the immunizing antigen are licensed to exit the GCs and to survive as long-lived plasma cells and/or memory B cells. Guiding B cells through these stochastic events is a subset of $CD4^+$ T helper cells, known as T follicular helper (T_{FH}) cells[2, 3, 4].

In secondary lymphoid organs, B and T cells are organized orderly into B-cell follicles and T-cell zones, based on gradients of CXCL13 and CCL19-CCL21 chemokines, respectively. Homing of T cells into B-cell follicles requires the concomitant up-regulation of the CXCL13-responding CXCR5 chemokine receptor, and the down-regulation of the CCL19-CCL21-binding CCR7 chemokine receptor. This preconditioning process occurs at the priming stage during the interaction between dendritic cells (DC) and naïve T cells[5]. T cells conditioned to enter B-cell follicles acquire a distinct transcriptional profile by up-regulating Bcl6, the canonical transcription factor of T_{FH} cells, and repressing the expression of Blimp1[6, 7, 8]. The $CXCR5^+Bcl6^+$ $CD4^+$ T cells, hereafter dubbed nascent T_{FH} cells, which appear as early as 2-3 days after viral infection or protein immunization, migrate to the T-B border[9, 10]. At this site, contiguous interaction between nascent $CXCR5^+Bcl6^+$ T_{FH} cells and cognate B cells allows for further maturation of T_{FH} cells[11]. Fully mature T_{FH} cells, hereafter dubbed GC T_{FH} cells, are crucial to support B-cell responses. GC T_{FH} cells are distinguishable from nascent T_{FH} cells by the elevated expression of multiple markers, including the PD-1 receptor[5, 12, 13].

The ICOS-ICOSL receptor-ligand pair is quintessential throughout T_{FH} development. Homozygous *ICOS* loss is found in patients suffering from common variable immunodeficiency with a concomitant decrease in $CXCR5^+$ memory T_{FH} cells[14, 15]. Similarly, $Icos^{-/-}$ and $Icosl^{-/-}$ mice have deformed GCs, impaired humoral response, and lack immunological memory[16, 17, 18, 19]. However, the molecular basis for why ICOS is so critical in T_{FH} cell development and function remains relatively unclear. To date, phosphoinositide-3-kinase (PI3K) is the only signaling molecule known to interact with ICOS[20, 21]. However, PI3K associates with, and signals from, a number of other cell surface receptors, including CD28 and CTLA-4[22, 23, 24]. Furthermore, several studies have revealed that disruption of the ICOS-PI3K interaction, or selective deletion of PI3K components from T cells, do not result in a complete phenocopy of $Icos^{-/-}$ knockout animals[25, 26, 27]. These studies implied that unknown molecules could potentially mediate ICOS-dependent, but PI3K-independent, signaling pathways.

Here, we have used a proteomic approach to identify novel ICOS interacting partners and explore their relevance in ICOS signals that control T_{FH} cell development and function. We demonstrate that the ICOS cytoplasmic tail harbors two novel evolutionarily conserved motifs. Proteomics and biochemical analyses revealed that the ICOS proximal (IProx) motif physically recruits a serine/threonine kinase, TBK1 (TANK-binding kinase 1). Although the early polarization of nascent T_{FH} cells was unperturbed, GC T_{FH} cells and B-cell responses were significantly impaired in the absence of the IProx motif, or upon TBK1 depletion in $CD4^+$ T cells. Intriguingly, the IProx motif was homologous to a conserved motif found in tumor necrosis factor receptor (TNFR)-associated factors, TRAF2 and TRAF3. As

disruption of the shared motif in TRAF2 and TRAF3 abolished their association with TBK1, we not only revealed the critical role of TBK1 in adaptive T cell immunity via its association with ICOS, but also discovered a TBK1-binding consensus sequence.

Results

Development of GC T_{FH} cells requires the IProx motif

Besides the PI3K-binding YxxM motif, the cytoplasmic tail of ICOS lacks known canonical motifs that mediate protein-protein interactions. To unveil other potential binding sites, we performed sequence alignments of the cytoplasmic tail in ICOS orthologs (Supplementary Fig. 1a). Intriguingly, this analysis revealed that, in addition to the PI3K-binding motif, there are two additional highly conserved motifs in the intracellular domain of ICOS (Fig. 1a). The finding of the YxxM motif as one of the three conserved motifs validated our bioinformatics search. The other two conserved motifs are the ^{170}SSSVHDPNGE^{179} motif and the ^{186}AVNTAKK^{193} motif. The conservation of these two motifs suggested that they have important function(s), and potentially the recruitment of other molecule(s) that may mediate downstream ICOS signaling.

We focused on the proximal ^{170}SSSVHDPNGE^{179} (IProx) motif. To examine the physiologic significance of this motif, we generated retroviral (RV) vectors that express wild-type ICOS (WT) or three ICOS mutants, *i.e.* replacement of the IProx motif by a string of 10 Ala substitutions (mIProx), mutation of the PI3K-binding site (Y181F; YF), and deletion of the cytoplasmic tail (amino acid residues 170-200; TL), respectively. The corresponding RV were used to reconstitute ICOS expression in *Icos*$^{-/-}$ TCR-transgenic SMARTA CD4$^+$ T cells. All transduced ICOS proteins displayed similar surface expression in the reconstituted cells (Supplementary Fig. 2a, 2b). Sorted transduced (GFP$^+$) cells were adoptively transferred into B6 recipient mice, and analyzed 7 days after an acute infection with LCMV Armstrong strain. As expected, *Icos*$^{-/-}$ SMARTA CD4$^+$ T cells reconstituted with WT differentiated into CXCR5$^+$SLAM^{lo} T_{FH} cells; in contrast, each of the three ICOS mutants failed to properly generate the CXCR5$^+$SLAM^{lo} T_{FH} cell population (Fig. 1b, c). Additionally, we also assessed the presence of GC T_{FH} cells, which express high amounts of PD-1. The differentiation of CXCR5$^+$PD1^{hi} GC T_{FH} cells was restored in *Icos*$^{-/-}$ SMARTA CD4$^+$ T cells reconstituted with WT, but remained significantly impaired upon reconstitution with each of the three mutants (Fig. 1d, e). With the exception of the TL mutant, we recovered similar numbers of transduced cells in all groups (Supplementary Fig. 3a), suggesting that the observed defects are not due to differences in T cell proliferation and/or cell death. Taken together, our data demonstrated that, in addition to the PI3K-binding motif, the IProx motif is also required for T_{FH} cell differentiation.

To further elucidate the physiologic relevance of the IProx motif in B-cell responses, we performed similar transfers of RV$^+$ *Icos*$^{-/-}$ SMARTA CD4$^+$ T cells into recipient mice with a CD4-specific conditional deletion of *Bcl6*. The CD4-Cre$^+$ *Bcl6*$^{fl/fl}$ recipient mice are intrinsically unable to generate T-dependent B cell immunity[6, 28]. Adoptive transferred mice were immunized with keyhole limpet hemocyanin (KLH)-conjugated LCMV gp61-80 peptide (KLH-gp61), and their responses were analyzed. The B-cell responses in these mice were fully dependent on the ability of transferred T cells to differentiate into GC T_{FH} cells

as mIProx, YF and TL mutants failed to restore this cell population (Supplementary Fig. 4a, 4c). As a benchmark for proper development of GC T_{FH} cells, the transfer of *Icos*$^{-/-}$ SMARTA CD4^{+} T cells reconstituted with WT supported the differentiation of Fas^{+}GL7^{+} GC B cells (Fig. 1f, g) and IgD^{-}CD138^{+} plasma cells (PC) in response to KLH-gp61 immunization (Fig. 1h, i). In sharp contrast, B cell differentiation was severely affected in the absence of a functional IProx motif, or PI3K-binding motif, or the complete absence of the ICOS intracellular tail, with GC B cell frequencies indistinguishable from the *Icos*$^{-/-}$ control (Fig. 1f-i). Moreover, the anti-KLH-gp61 IgG response was greatly diminished in mice receiving *Icos*$^{-/-}$ CD4^{+} T cells reconstituted with IProx, YF or TL mutants (Fig. 1j). The quantity of the antigen-specific IgG response was significantly and severely impaired in the absence of either IProx-dependent or PI3K-dependent ICOS signaling (Fig. 1k, 1l). Therefore, the development of these antigen-specific T-dependent B-cell responses required complete ICOS signaling involving both the IProx and YxxM motifs. These data establish that the IProx motif is required for the *in vivo* differentiation of GC T_{FH} cells.

TBK1 physically interacts with the IProx motif

To identify putative molecule(s) that could bind to the IProx motif, we undertook an unbiased proteomic approach using SILAC, which allows for quantitative comparative measurement of proteins. We analyzed the proteomes of ICOS immunoprecipitations (IPs) obtained from cells expressing WT or mIProx following anti-CD3 plus –ICOS costimulation. One cytosolic protein, TANK-binding kinase 1 (TBK1), a non-canonical member of the IκB kinase (IKK) family, had the highest difference in binding ratio (~8-fold) between WT- *vs.* mIProx-expressing cells (Table 1). TBK1 is critically required for production of Type I interferon by innate immune cells[29]. However, the role of TBK1 in T cells has not been pinpointed.

To validate the proteomic data, we performed a co-IP analysis and found that ICOS co-immunoprecipitated with endogenous TBK1 in pre-activated primary CD4^{+} T cells upon restimulation with anti-CD3 plus anti-ICOS (Fig. 2a). Moreover, TBK1 phosphorylated on the activating residue (Ser172) was detected in ICOS immunoprecipitation, suggesting that ICOS can recruit the active form of TBK1. Subsequently, we transfected Jurkat T cells with WT, mIProx, YF or TL mutant, and analyzed the presence of TBK1 in ICOS IPs from stimulated cells. WT interacted strongly with endogenous TBK1, but the interaction was substantially diminished in cells expressing mIProx (Fig. 2b, 2c), consistent with the proteomic data. Mutation of tyrosine residue (YF) abolished the binding of p85α (the regulatory subunit of PI3K) without affecting the ICOS-TBK1 interaction, and binding of p85α to ICOS was not impaired in mIProx (Fig. 2b, 2c). In addition, we determined that TBK1 associated only with ICOS, but not with the closely related CD28 and CTLA-4 (Fig. 2d), demonstrating that this signaling pathway is unique to ICOS.

To explore the physiologic relevance of ICOS-TBK1 interaction, we examined human GC T_{FH} cells. There was basal interaction between ICOS and TBK1 in unstimulated human GC T_{FH} cells (Fig. 2e). The TBK1 interaction with ICOS was further strengthened upon stimulation with anti-CD3 plus anti-ICOS (Fig. 2e), suggesting that the ICOS-TBK1 interaction in GC T_{FH} cells is inducible via inputs from TCR and ICOS signals. Taken

together, these data indicate that ICOS physically interacts with active TBK1 via the conserved IProx motif in T_{FH} cells.

Development of GC T_{FH} cells requires TBK1

Since we demonstrated that the IProx motif is required for T_{FH} development (Fig. 1), and that this motif physically interacts with TBK1 (Fig. 2), we hypothesized that TBK1 plays a role in the differentiation of T_{FH} cells. To test this hypothesis, we used an RNAi knockdown strategy. Ag-specific SMARTA $CD4^+$ T cells were retrovirally transduced with shRNA targeting the *Tbk1* gene (sh*Tbk1*-1 or sh*Tbk1*-2, Supplementary Fig. 2c). In parallel, we used a control shRNA (shControl) and an shRNA targeting *Icos* (sh*Icos*), as negative and positive controls, respectively. Transduced SMARTA $CD4^+$ T cells were adoptively transferred into B6 mice and analyzed 7 days post-LCMV infection to assess the impact of TBK1 depletion on GC T_{FH} development.

Depletion of ICOS in SMARTA $CD4^+$ T cells significantly reduced the $CXCR5^+SLAM^{lo}$ T_{FH} cell population, as well as the $CXCR5^+PD1^{hi}$ and $CXCR5^+GL\text{-}7^+$ GC T_{FH} cell populations (Fig. 3a – 3f). Importantly, knockdown of *Tbk1* in Ag-specific $CD4^+$ T cells also significantly impaired the full development of GC T_{FH} cells (Fig. 3a – 3f), demonstrating that TBK1 is critical for the full commitment of T_{FH} differentiation. The *Tbk1* transcript was reduced by ~75% *in vivo* in sorted sh*Tbk1*-1^+ or sh*Tbk1*-2^+ cells (Supplementary Fig. 2e, 2g), and they accumulated comparably to control cells *in vivo* (Supplementary Fig. 3b).

To assess the physiologic relevance of TBK1 in T-dependent B-cell responses, we employed $CD4\text{-}Cre^+$ $Bcl6^{fl/fl}$ mice immunized with KLH-gp61 and examined the GC and antibody responses. Differentiation of $CXCR5^+PD1^{hi}$ GC T_{FH} cells was severely impaired in the presence of sh*Tbk1*-1^+ or sh*Tbk1*-2^+, consistent with the results obtained in acute viral infection (Supplementary Fig. 4b, 4d). Fas^+PNA^+ GC B cell frequencies were significantly reduced when TBK1 was depleted in SMARTA $CD4^+$ T cells (Fig. 3g, 3h). Anti-KLH-gp61 specific IgG responses were also significantly impaired when ICOS or TBK1 was depleted (Fig. 3i – 3k). Anti-KLH-gp61 IgG titers were ~10-fold lower in the absence of an intact ICOS-TBK1 signaling pathway (Fig. 3j). Concomitantly, the architecture of PNA^+ GCs was severely compromised in mice receiving sh*Icos*$^+$, sh*Tbk1*-1^+ or sh*Tbk1*-2^+ cells compared to controls (Fig. 3l). Taken together, TBK1 in $CD4^+$ T cells is required to support T_{FH} differentiation, the development of GC and antigen-specific T-dependent IgG responses.

IProx is dispensable for nascent T_{FH} cell development

The complete programming of T_{FH} cells is a multistep process involving T cell-DC interaction at the early stage and T-B cell interaction at a later phase[9, 30, 31]. To assess the importance of the IProx motif in the differentiation of nascent T_{FH} cells, we carried out a similar reconstitution experiment, and performed the analysis earlier, *i.e.*, 3-day post-infection. As expected, $Icos^{-/-}$ SMARTA $CD4^+$ T cells reconstituted with WT were able to differentiate into $CXCR5^+Bcl6^+$ nascent T_{FH} cells. However, to our surprise, $Icos^{-/-}$ SMARTA $CD4^+$ T cells reconstituted with the mIProx were equally capable of polarizing into nascent T_{FH} cells (Fig. 4a, 4b). Additionally, the Bcl6 protein expression was

comparable between T cells reconstituted with WT or mIProx (Fig. 4c), indicating that the early expression of Bcl6, and potentially its regulatory functions, is independent of the IProx motif.

Down-regulation of CD25 is an additional characteristic of early T_{FH} programming[9]. The $CXCR5^+CD25^{lo}$ nascent T_{FH} population was comparable between *Icos*$^{-/-}$ SMARTA $CD4^+$ T cells reconstituted with WT or the mIProx (Fig. 4d, 4e). However, mice receiving the *Icos*$^{-/-}$ SMARTA $CD4^+$ T cells reconstituted with the YF or TL mutants had reduced nascent T_{FH} cells identified by $CXCR5^+Bcl6^+$ or $CXCR5^+CD25^{lo}$ phenotyping (Fig. 4d, 4e) and also expressed lower levels of Bcl6 (Fig. 4c). Furthermore, we performed immunofluorescence histology enumerating the congenic $CD45.1^+$ *Icos*$^{-/-}$ SMARTA T cells reconstituted with WT or mIProx in B-cell follicles. There was no significant difference between cells reconstituted with WT or mIProx in B-cell follicles (Fig. 4f), consistent with nascent T_{FH} differentiation and migration being independent of the ICOS-TBK1 pathway. Thus, nascent T_{FH} differentiation occurs in the absence of the IProx motif. However, the subsequent maturation of T_{FH} cells is blocked in the absence of this ICOS-mediated pathway. Taken together, these results shows that the ICOS-PI3K pathway regulates the very early stage of T_{FH} polarization, whereas the signaling emanating from the IProx motif is critically required for the progression from nascent T_{FH} to GC T_{FH} cells.

TBK1 is dispensable for nascent T_{FH} cell development

To further dissect the role of TBK1 in T_{FH} development, we tracked the development of the nascent T_{FH} cells in TBK1-depleted T cells at an earlier time point, *i.e.* 3-day post-infection. Knockdown of *Icos* in SMARTA $CD4^+$ T cells significantly impeded the differentiation of nascent T_{FH} cell differentiation, compared to control (Fig. 5a, 5b). The $CXCR5^+Bcl6^+$ nascent T_{FH} cell differentiation was not affected in cells containing sh*Tbk1*-1 or sh*Tbk1*-2 (Fig. 5a, 5b). Commensurate with this, there was no significant difference in the expression level of Bcl6 protein between control cells and sh*Tbk1*-1^+ or sh*Tbk1*-2^+ cells (Fig. 5c). Analyses of the nascent T_{FH} cells with additional markers, *i.e.* $CXCR5^+CD25^{lo}$ and $CXCR5^+SLAM^{lo}$, gave comparable results (Fig. 5d – 5e, Supplementary Fig. 5a, 5b). Furthermore, we did not observe any difference in the levels of CXCR5, TCR, CD28 or CD40L (Supplementary Fig. 5c – 5f). The *in vivo* knockdown efficiency of *Tbk1* mRNA 3 days post-infection was ~80 % (Supplementary Fig. 2d, 2f). In agreement with the mIProx reconstitution data (Fig. 4), knockdown of *Tbk1* in SMARTA $CD4^+$ T cells did not interfere with the early differentiation of nascent T_{FH} cells. Therefore, signals mediated by TBK1 binding to the IProx motif license nascent T_{FH} cells to enter the GC phase of T_{FH} development.

Molecular basis of the ICOS-TBK1 interaction

Because the ICOS-PI3K and ICOS-TBK1 pathways exhibit distinctive behavior with regard to the priming and GC stages of T_{FH} development, we hypothesized that the two pathways are activated by different stimulating signals. To investigate this hypothesis, we stimulated $CD4^+$ T cells in the presence of anti-CD3 alone, anti-ICOS alone, or the combination of both, to mimic TCR signaling, ICOS-ICOSL signaling, or the simultaneous activation of both signals, respectively. We then analyzed the association of ICOS with either p85α or

TBK1 under these conditions. In the absence of stimulation, ICOS did not co-IP with p85α, but the ICOS-p85α association was rapidly induced by all three forms of stimulation (Fig. 6a). Strikingly and in stark contrast, TBK1 co-immunoprecipitated with ICOS only when the cells were costimulated with anti-CD3 plus anti-ICOS, but not under conditions of no stimulus or when single stimuli were applied (Fig. 6a). These results indicate that combined signaling from the TCR and ICOS is required to induce ICOS-TBK1 association. Additionally, in $CD4^+$ T cells, the phosphorylation of TBK1 was induced only in the presence of a strong anti-CD3 plus anti-ICOS signal (Fig. 6b), supporting the notion that strong TCR stimulation favors a TBK1-dependent signal to drive the differentiation of GC T_{FH} cells[32]. Thus, the requirement for activation of the ICOS-TBK1 signaling is more stringent than that for the ICOS-PI3K pathway in that it requires two simultaneous signals provided by the strong cognate interaction between T cells and APCs.

TBK1 transduces pivotal signals from TNFR and TLR molecules[29]. TRAF proteins, particularly TRAF2, TRAF3 and TRAF5, but not TRAF6, can physically interact with TBK1 to mediate the downstream effector functions[33, 34], although the TBK1-binding motif in TRAFs has not been defined. We were not able to detect co-immunoprecipitation of TRAF2, TRAF3 or TRAF5 with ICOS in T cells, consistent with the fact that ICOS does not belong to the TNFR or TLR superfamilies (Supplementary Fig. 6). Additionally, IKKε, which forms a complex with TBK1[35, 36], was also absent from the immunoprecipitated ICOS signalosome (Supplementary Fig. 6), reinforcing the possibility that the ICOS-TBK1 pathway is mechanistically distinct from the TNFR or TLR pathways. We speculated that, instead of recruiting TBK1 via TRAFs, perhaps ICOS itself might contain a motif shared with TBK1-binding TRAF proteins. To test this idea, we performed a BLASTp analysis comparing human ICOS cytoplasmic tail and full-length TRAF2 and TRAF3. To our surprise, this analysis revealed a significant homology between the IProx motif and a region of TRAF2 and TRAF3 known as the “serine tongs”[37] (Fig. 6c). This region (SSSxxxPxGD/E) is found in TRAF2, TRAF3 and TRAF5, which are the known TRAF to bind TBK1, but not in TRAF4 and TRAF6 (Fig. 6c). Additionally, this extended “serine tongs” motif is also well conserved among TRAF2 and TRAF3 orthologs throughout evolution (Supplementary Fig. 1b, 1c).

The homology between ICOS and TRAF proteins suggested that the shared motif is a consensus TBK1-binding motif. To validate this notion, we substituted the corresponding region in TRAF2 (residues 453-462) and TRAF3 (residues 518-527), with a string of 10 alanine residues and examined the interaction of these TRAF mutants with TBK1. While TBK1 interacted strongly with WT TRAF2 (Fig. 6d) and TRAF3 (Fig. 6e), its association with the corresponding mutated TRAFs was strongly reduced, similar to the defective association of TBK1 with the mIProx (Fig. 2b). Therefore, these results support the notion that the IProx motif by itself acts as a TBK1-binding site on ICOS, thus bypassing the requirement of TRAF molecules as intermediary partners.

Discussion

$CD4^+$ T cells undergo sequential phases of differentiation and maturation to become mature *bona fide* GC T_{FH} cells. ICOS signaling plays a critical role in T_{FH} cell development, and

the only protein so far known to interact with the cytoplasmic tail of ICOS in an inducible manner is PI3K. However, previous studies demonstrated that several ICOS-mediated T cell functions are independent of PI3K signaling[25, 26, 27], implying the existence of additional ICOS signaling pathways. Here, we have unraveled a signaling pathway emanating from ICOS, which is critical for the full maturation of GC-residing T_{FH} cells. Specifically, we have: identified a previously unknown, evolutionarily conserved membrane proximal ICOS motif, IProx, that is required for T_{FH} development and function; identified TBK1 as an activation-induced interacting partner of this motif; demonstrated that the recruitment of TBK1 to ICOS is required for the development of GC T_{FH} cells while being dispensable for the differentiation of nascent T_{FH} cells; and identified a TBK1-binding consensus sequence that is shared between the IProx motif and TRAF2/3 molecules.

TBK1 is essential for the production of Type I interferon in innate immune cells[35, 36]. Additionally, TBK1 also plays a role in non-immune cells[38], in B cells[39], as well as in immune responses to DNA vaccines[40]. TBK1 was found to interact with TRAF2 and activate NF-κB signaling[41]. Subsequently, TRAF3, but not TRAF6, was shown to bind TBK1[33, 42]. However, the actual motif in TRAF2 and TRAF3 required for TBK1 binding has not been definitively mapped. Here, we mapped the TBK1-binding site to the IProx motif and found that this motif is also present in TBK1-binding TRAF proteins. This TRAF motif, termed a “serine tongs” motif, was initially proposed to function as a TRAF2-binding site for the cytoplasmic domain of CD40[37], but subsequent analyses failed to corroborate this notion[43]. Thus, the role of the highly conserved “serine tongs” motif in TRAF2 and TRAF3 has remained controversial. Our findings strongly suggest that the SSSxxxPxGD/E IProx motif represents the canonical TBK1-binding sequence.

Initial signals required for the polarization of nascent T_{FH} cells include CD28-B7[44, 45] and ICOS-ICOSL[9, 46]. Previous studies have circumstantially linked these early events to the PI3K-mediated ICOS pathway[9, 25]. Moreover, ICOS stimulation induces the interaction of PI3K with intracellular osteopontin, resulting in the latter protein interacting with Bcl6 and protecting it from degradation. Ablation of intracellular osteopontin led to the failure of Bcl6 maintenance as early as three days post protein immunization[47]. Our finding that mutation of the PI3K-binding site in ICOS hindered the polarization of nascent T_{FH} cells and significantly compromised early Bcl6 protein expression is fully consistent with the above studies.

Our study reveals a new molecular pathway, *i.e.* the TBK1-dependent pathway mediated by the IProx motif, which functions to drive the differentiation of T cells from the nascent T_{FH} stage to the mature GC T_{FH} stage. Nascent T_{FH} cells are the precursors of *bona fide* GC T_{FH} cells. Only upon contact with cognate B cells do these nascent T_{FH} cells receive additional maturation signals to become $CXCR5^{+}PD1^{hi}$ GC T_{FH} cells. GC T_{FH} cells fail to develop in the absence of B cells[5, 6, 11], upon B cell-specific conditional deletion of ICOSL[48], or following anti-ICOSL antibody blockade[9], indicating that ICOS-ICOSL engagement mediated by cognate T-B cell interaction is essential for the continuous maturation of these interacting cells. Recent data have also shown that ICOS-driven motility, which promotes T_{FH} cell migration deep into the follicular parenchyma, can also be dependent on ICOS-

coupled PI3K-mediated signaling triggered by ICOSL present on bystander follicular B cells, which do not present cognate antigen[49].

Our findings demonstrating a role for distinct ICOS-linked signaling modules in full T_{FH} differentiation can potentially unify these seemingly opposing observations, since we have showed that while either TCR or ICOS stimulation alone can induce the association of ICOS with PI3K, a combination of both signals was required to recruit and activate TBK1. Therefore, it could be argued that upon encountering B cells expressing cognate peptide-MHC and ICOSL, ICOS-TBK1 signaling, possibly in conjunction with ICOS-PI3K pathway, induces the maturation process of nascent T_{FH} cells. Upon this differentiation step, mature T_{FH} cells could migrate into the follicular parenchyma through serial interactions with bystander follicular B cells in a manner dependent on the ICOS-ICOSL interaction[49], but independent of TCR signals, which would be sufficient to trigger the ICOS-PI3K signaling pathway. Consistently, we found that there was no defect in early T_{FH} migration in the absence of ICOS-TBK1 pathway, but the nascent immature T_{FH} cells infiltrated into B-cell follicles are incapable of supporting B cell maturation and GC development. Therefore, there is a bifurcation in functionality between the IProx-motif dependent ICOS-TBK1 pathway and the ICOS-PI3K pathway. Our data demonstrate that both pathways are essential, independently, for T_{FH} differentiation, GC development and IgG response.

Ab production is a double-edged process. $CD4^+$ T_{FH} cells are endowed with the ability to positively support the maturation of B cells producing Abs with the highest affinity for the immunizing antigen, while counter-selecting for B cells expressing self-reactive Abs. Here, we showed that ICOS regulates a novel TBK1-dependent signaling pathway, which is exquisitely required to allow the commitment to become fully functional GC T_{FH} cells. Therefore, our findings expand the essential roles of TBK1 to antigen-specific $CD4^+$ T cell immunity. Strategic manipulations of these ICOS-dependent pathways could lead to better vaccine design and treatment of autoimmune diseases.

Online Methods

Antibodies (Abs) and reagents

Monoclonal Abs specific for human CD3 (clone OKT3), and mouse CD3 (clone 145-2C11), -CD28 (clone 37.51), -CTLA-4 (clone UC10-4B9) or -ICOS (clone C398.4A) were purchased from Biolegend CA, as was phycoerythrin-conjugated anti-CD150/SLAMf1 (clone TC15-12F12.2). Fluorophore-conjugated anti-CD4 (mouse: clone RM4-5; human: clone RPA-T4), -CD8a (clone 53-6.7), -CD19 (mouse: clone eBio1D3; human: clone HIB19), -CD25 (clone PC61), -CD40L (clone MR1), -CD44 (clone IM7), -CD45.1 (clone A20), -CD62L (clone MEL-14), -GL7 (clone GL-7), -IgD (clone 11-26) and -PD1 (mouse: clone J43; human: clone J105) Abs were obtained from eBioscience, CA. Anti-mouse CXCR5 (mouse: clone 2G8; human: clone RF8B2), biotinylated anti-CD138 (clone 281-2), FITC-conjugated TCR β-chain (H57-597), phycoerythrin-conjugated anti-Fas/CD95 (clone Jo2) and allophycocyanin-conjugated anti-mouse Bcl6 (clone K112-91) were procured from BD Biosciences, CA. FITC-conjugated PNA was purchased from Vector Laboratories, CA. Monoclonal anti-TBK1 (#3013), -phospho-TBK1 (Ser172) (clone D52C2, #5483), -TRAF2 (#4712), -TRAF3 (#4729), p-ERK1/2 (T202/Y204) (clone E10, #9106) and -IKKε (#2690)

Abs were obtained from Cell Signaling Technology, MA. Monoclonal anti-p85α (sc-1637), -ERK2 (sc-1647) and -TRAF5 (sc-7220) were purchased from Santa Cruz Biotechnology, CA. Recombinant IL-2 and IL-7 cytokines were obtained from Biolegend, CA.

Plasmids

Plasmids of full-length human and mouse *Icos* were generated via PCR amplification and cloned into the pMIG retroviral vector. FLAG-tagged TRAF2 and TRAF3 clones were previously described[50]. Point mutations in *Icos*, *Traf2* and *Traf3* cDNAs were generated using Quikchange II Site-directed Mutagenesis Kit (Agilent Technologies, CA). Mutation of the IProx motif, mIProx (^{170}SSSVHDPNGE^{179} to ^{170}AAAAAAAAAA^{179}) was generated using overlapping PCR. The tailless *Icos* (TL) mutant was generated via PCR amplification by in-frame joining of amino acid 1-170 of ICOS to a flexible linker, LESGGGG, to stabilize its surface expression. Short hairpin RNA (shRNA) targeting the mouse *Tbk1* gene (sh*Tbk1*-1: 5′-AAGACATAAAGTGCTTATTATG-3′, sh*Tbk1*-2: 5′-ACTAATCAGTGTTTCGATAT-3′) and *Icos* gene (5′-TTCAGTTAATATGGTTTACTAT-3′) were amplified via PCR and cloned into an LMP plasmid as previously described[6, 9, 51].

Mice and primary cell cultures

C57BL/6 (B6), TCR-transgenic SMARTA B6 mice expressing a TCR transgene recognizing the immunodominant MHC class II-restricted LCMV epitope GP61-80, *Icos*$^{-/-}$ SMARTA, CD45.1^{+} *Icos*$^{-/-}$ SMARTA and CD4-Cre X *Bcl6*$^{fl/fl}$ mice were housed and maintained under specific pathogen-free conditions, and manipulated according to guidelines approved by the LJI Animal Care Committee. Mice of both sexes were used at 6 – 15 weeks of age. No statistical method was used to estimate the sample size. No pre-established inclusion/exclusion criteria were used for the analysis. Mice were randomly selected for adoptive transfer experiments. Investigators were blinded from the group allocation when assessing the outcome. CD4^{+} T cells were isolated by a CD4 negative selection kit (Miltenyi Biotec, Germany), and cultured in RPMI-1640 medium (Life Technologies, CA) supplemented with 10% heat-inactivated fetal bovine serum, 2 mM glutamine, 1 mM sodium pyruvate, 1 mM MEM nonessential amino acids, and 100 U/ml each of penicillin G and streptomycin (Life Technologies, CA).

Isolation of human GC T_{FH} cells

Human tonsils were obtained from the National Disease Resource Interchange. Informed consent was obtained from all donors. Tonsils were homogenized using wire mesh and passed through a cell strainer to make a single-cell suspension. Mononuclear cells were isolated using Histopaque 1077 (Sigma-Aldrich, MO). All protocols were approved by the La Jolla Institute for Allergy and Immunology (LJI) and National Disease Resource Interchange. 500 × 10^{6} mononuclear cells were enriched with biotinylated anti-human PD1 (clone J105; eBiosciences, CA) at 0.20 μg per million cells, followed by strepavidin-conjugated microbeads (Miltenyi Biotec, Germany). Enriched cells were > 80 % GC T_{FH} based on the expression of CXCR5 and PD1 by flow cytometry. Enriched GC T_{FH} cells were left unstimulated or stimulated with 10 μg/ml of anti-CD3 (clone OKT3) and -ICOS (clone C398.4A) Abs in the presence of a cross-linking Ab for 2 min. Cell lysis in 1%

NP-40 lysis buffer (50 mM Tris-HCl, pH7.4, 50 mM NaCl, 5 mM EDTA), immunoprecipitation, and immunoblotting were carried out as previously described[22, 23].

Retroviral production, cell transfers and viral infections

ICOS-expressing retroviral plasmids and shRNA-carrying retroviral plasmids (LMP) DNAs were transfected into Plat-E cell lines for virion production, as previously described[6, 9, 51]. Cultured supernatants were obtained 1 d later, filtered through 0.45 μm syringe filters and spin-infected into *in vitro* activated SMARTA or *Icos*$^{-/-}$ SMARTA CD4^{+} T cells by centrifugation at 2,000 rpm for 90 min at 37 °C. Following two consecutive rounds of retroviral infection, CD4^{+} T cells were maintained and expanded in the presence of 10 ng/ml IL-2 for 2 d, and rested subsequently in the presence of 2 ng/ml IL-7 overnight prior to cell sorting.

Retrovirally transduced GFP^{+} or Ametrine^{+} cells (5×10^5, 2.5×10^4, 2.0×10^4 cells for 3–, 7– and 10–day experiments, respectively) were transferred into recipient mice by i.v. injection. LCMV Armstrong viral stocks were prepared and quantified as previously described[6, 9, 51]. Five $\times 10^5$ and 2×10^5 plaque-forming units (PFU) per mouse were inoculated i.p. for 3– and 7–day experiments, respectively.

Protein immunizations and B-cell responses

For reconstitution study, 2×10^5 retrovirally transduced GFP^{+} cells were transferred into CD4-Cre × *Bcl6*$^{fl/fl}$ recipients by i.v. injection. A total of 20 μg of LCMV gp61-80 peptide (GLNGPDIYKGVYQFKSVEFD) conjugated to keyhole limpet hemocyanin (KLH) was resuspended in alum and 2 μg LPS for i.p. injection. Spleens were obtained 10 days post-immunization for B cell analyses. For shRNA knockdown study, 2×10^5 retrovirally transduced Ametrine^{+} cells were transferred into CD4-cre × *Bcl6*$^{fl/fl}$ recipients by i.v. injection. A total of 30 μg of LCMV gp61-80 peptide conjugated to keyhole limpet hemocyanin (KLH) was resuspended 1:1 in AddaVax (Invivogen Inc., San Diego CA) for footpad injection. Popliteal lymph nodes were obtained 10 days post-immunization for B cell analyses and immunohistochemistry analyses.

Flow cytometry

Single cell suspensions were prepared by a gentle mechanical disruption of spleens. The triple-step CXCR5 stains and intracellular Bcl6 stains were described previously[6, 9, 51]. All FACS samples were acquired with an LSRII (BD Biosciences) immediately after the staining protocol, and analyzed with FlowJo software.

Immunofluorescence staining of germinal centers

Popliteal lymph nodes from mice immunized with KLH-gp61 were snap frozen in OCT medium (Sakura Finetek, USA), and 6–8 μm sections were prepared using a cryostat. LN sections were fixed with acetone, and stained with biotinylated-PNA followed by streptavidin conjugated to Alexa Fluor 555 (Life Technologies, CA), anti-IgD Ab conjugated to FITC, anti-CD4 Ab conjugated to Alexa Fluor 647 and DAPI to reveal the germinal centers, B cell zone, T cell zone and nuclei, respectively. Sectioned were fixed with mounted

with ProLong gold antifade reagent (Life Technologies, CA), and imaged by Zeiss AxioScan Z1 Slide Scanner.

Immunofluorescence staining for localization study

Congenic CD45.1$^+$ *Icos*$^{-/-}$ SMARTA T cells were reconstituted with retroviral vector expressing WT ICOS or mIProx. 2 × 10^6 retrovirally transduced cells were sorted and transferred into CD45.2$^+$ B6 recipients by i.v. injection. Five × 10^5 PFU of LCMV Armstrong were inoculated i.p. Spleens were snap frozen in OCT medium (Sakura Finetek, USA), and 6–8 μm sections were prepared using a cryostat. Spleen sections were fixed with acetone and stained with biotinylated-anti-CD45.1 mAb followed by streptavidin conjugated to Alexa Fluor 555 (Life Technologies, CA), anti-IgD Ab conjugated to FITC, anti-CD4 Ab conjugated to Alexa Fluor 647 and DAPI, to reveal the transferred T cells, B cell area, T cell zone and nuclei, respectively. Sectioned were fixed with mounted with ProLong gold antifade reagent (Life Technologies, CA), and imaged by Zeiss AxioScan Z1 Slide Scanner. To analyze the CD45.1$^+$ SMARTA T cells in B-cell follicles, first, a perimeter was manually drawn around the border between the T cell zone and B cell zone in a white pulp using a composite image of the CD4 and IgD stains, respectively. To identify SMARTA T cells, image of the CD45.1 stain was first masked using Otsu's method. An erosion and then dilation was performed on the cell mask, and objects smaller than cells removed from the mask. Cells inside the T-B border region were counted and normalized to the B cell areas. This was process was repeated for all identifiable B-cell follicles in each spleen section.

Anti-KLH-gp61-80 ELISA

Sera were obtained through retro-orbital bleeding 10 days after protein immunization with KLH-gp61 plus adjuvants. 96-well PolySorp microtiter plates (Nunc, Thermo Fisher Scientific, MA) were coated overnight with KLH-gp61-80 in PBS. Sera were serially titrated at 1:3 and incubated with KLH-gp61-80 for 2 h. After incubation of sample serum, plates were washed and then incubated with horseradish peroxidase–conjugated goat antibody to mouse IgG, followed by colometric detection with tetramethylbenzidine substrate solution (172-1068; Bio-Rad, CA). Reaction was terminated using 2N sulfuric acid and the absorbance was read at 450 nm. Data were analyzed by two methods, endpoint titer and area under the curve (AUC). Endpoint titers of log transformed data were calculated as the interpolated serum dilution at 0.1 OD above background. AUC analysis better accounts for both the quantity of the IgG, as it accounts for the shape of the curve. AUC total peak area above baseline calculations (Graphpad Prism 6.0) were done for each individual sample, log transformed.

Immunoprecipitation and immunoblotting

The human leukemic Jurkat T cell line, JTAg, was previously described[22, 23], and the HEK 293T cell line was obtained from ATCC. These cell lines have not been recently STR profiled but tested negative for mycoplasma contamination. JTAg cells in logarithmic growth phase were transfected with plasmid DNAs by electroporation and incubated for 24 h. Transfection of HEK293T cells was carried out via liposomes-mediated transfection with plasmid DNAs. For experiments using primary mouse T cells, purified CD4$^+$ T cells were activated *in vitro* with anti-CD3 (clone 145-2C11, 5 μg/ml) and anti-CD28 (clone 37.51, 5

μg/ml) for 48 h prior to resting in the presence of IL-2 for another 48 h. Transfected JTAg cells and preactivated mouse $CD4^+$ T cells were stimulated with 10 μg/ml of anti-CD3 and anti-ICOS (clone C398.4A) Abs in the presence of a cross-linking Ab for 2 min. Cell lysis in 1% NP-40 lysis buffer (50 mM Tris-HCl, pH7.4, 50 mM NaCl, 5 mM EDTA), immunoprecipitation, and immunoblotting were carried out as previously described[22, 23]. The intensity of bands was measured using the ImageJ software (NIH). To determine the ratio of TBK1 to p85α, the band intensity on IP blots and WCL blots were measured for TBK1 and p85α, respectively, and the ratio was expressed as (IP TBK1)/(WCL TBK1): (IP p85α)/(WCL p85α).

Isolation of mRNA, cDNA synthesis and real-time PCR

Total RNA was extracted from sorted $CD4^+$Ametrine$^+$ cells using the RNeasy kit (Qiagen, Germany). RNA was used to synthesize cDNA by the iScript synthesis kit (Bio-Rad, CA). Gene expression was determined using real-time PCR with iTaq SYBR Green (Bio-Rad, CA) in the presence of the following primer sets for mouse *Icos* (Forward: 5′-ACTGGTGATCTCTATGCTGTCA-3′; Reverse: 5′-TTCTGGAAGTCCATACGCATTG-3′), *Tbk1* (Forward: 5′-TGACCCACCTCCTTTTCAAG-3′; Reverse: 5′-TTAGGGTCATGCACACTGGA-3′) and the housekeeping gene β-actin (*ACTB*)[22, 23]. Relative gene expression levels were determined in duplicates, calculated using the $2^{-\Delta\Delta Ct}$ method and normalized to the level of *ACTB*.

SILAC and proteomic analysis

Plasmids expressing WT ICOS and mIProx were transfected into JTAg cells as described above in regular RPMI-1640 medium or medium supplemented with ^{13}C, ^{15}N labeled lysine and arginine for SILAC labeling[22]. FACS-sorted GFP^+ transduced cells were stimulated with anti-CD3 plus anti-ICOS Abs in the presence of a cross-linking for 2 min. 300 μg of the protein mixture derived from WT and mutant cell lysate were immunoprecipitated with anti-ICOS Ab, and mixed at a 1:1 ratio. Immunoprecipitates were subjected to an on-bead digestion protocol. The proteins were reduced with 100 mM Tris-HCl/8 M urea/5 mM tris(2-carboxyethyl)phosphine, and alkylated with 10 mM iodoacetamide. The solution was diluted 1:4 and digested with 1 μg of trypsin at 37ºC overnight. Digestion was terminated by adding 2% formic acid, and the resulting peptides were subjected to 6-step MudPIT LC-MS/MS analysis as described previously[52]. MS analysis was performed using an LTQ-Orbitrap Velos mass spectrometer (Thermo Fisher). A cycle of one full-scan mass spectrum (300-1800 m/z) at a resolution of 60,000 followed by 20 data dependent MS/MS spectra at a 35% normalized collision energy was repeated continuously throughout each step of the multidimensional separation. The experiments were biologically repeated in four replicates, including medium isotope type swapping (heavy or light) between WT and mutant cells.

The mass spectrometric data were analyzed via the Integrated Proteomics Pipeline - IP2 (Integrated Proteomics Applications, Inc., San Diego, CA. http://www.integratedproteomics.com/) using ProLuCID[53], DTASelect2[54] and Census_ENREF_61[55]. The tandem mass spectra were searched against EBI IPI human target/decoy protein database. The protein false discovery rates were controlled below 1% for each sample. In ProLuCID database search, the cysteine carboxyamidomethylation was

set as a stable modification. The peptide quantification was performed by Census software, in which the isotopic distributions for both the unlabeled and labeled peptides were calculated and this information was then used to determine the appropriate m/z range from which to extract ion intensities.

Statistical analysis

Statistical analyses were performed using the non-parametric Mann-Whitney U test for the comparison of two groups, and ANOVA with *post-hoc* Tukey's corrections for the comparison of more than two groups. $P < 0.05$ was considered as statistically significant.

Supplementary Material

Refer to Web version on PubMed Central for supplementary material.

Acknowledgments

The authors would like to acknowledge lab members in the Altman and Crotty laboratories for helpful discussion. We are indebted to the excellent services provided by the Flow Cytometry Core Unit, the Microscopy Unit, and the Animal Husbandry Unit at LJI. The authors are also grateful to the imaging and bioinformatics services provided by P. Beemiller, who assisted in computational analyses of immunohistochemistry using Matlab. We acknowledge clinical samples provided by the National Disease Resource Interchange. This is publication number 1794 from the La Jolla Institute for Allergy and Immunology. This work was supported by NIH grants CA35299 (AA), AI109976, AI063107, and AI072543 (SC). KFK was supported by Young Investigator Award #270056 from the Melanoma Research Alliance.

References

1. Victora GD, Nussenzweig MC. Germinal centers. Annu Rev Immunol. 2012; 30:429–457. [PubMed: 22224772]
2. Crotty S. A brief history of T cell help to B cells. Nat Rev Immunol. 2015; 15(3):185–189. [PubMed: 25677493]
3. Ramiscal RR, Vinuesa CG. T-cell subsets in the germinal center. Immunol Rev. 2013; 252(1):146–155. [PubMed: 23405902]
4. Craft JE. Follicular helper T cells in immunity and systemic autoimmunity. Nat Rev Rheumatol. 2012; 8(6):337–347. [PubMed: 22549246]
5. Haynes NM, Allen CD, Lesley R, Ansel KM, Killeen N, Cyster JG. Role of CXCR5 and CCR7 in follicular Th cell positioning and appearance of a programmed cell death gene-1high germinal center-associated subpopulation. J Immunol. 2007; 179(8):5099–5108. [PubMed: 17911595]
6. Johnston RJ, Poholek AC, DiToro D, Yusuf I, Eto D, Barnett B, et al. Bcl6 and Blimp-1 are reciprocal and antagonistic regulators of T follicular helper cell differentiation. Science. 2009; 325(5943):1006–1010. [PubMed: 19608860]
7. Nurieva RI, Chung Y, Martinez GJ, Yang XO, Tanaka S, Matskevitch TD, et al. Bcl6 mediates the development of T follicular helper cells. Science. 2009; 325(5943):1001–1005. [PubMed: 19628815]
8. Yu D, Rao S, Tsai LM, Lee SK, He Y, Sutcliffe EL, et al. The transcriptional repressor Bcl-6 directs T follicular helper cell lineage commitment. Immunity. 2009; 31(3):457–468. [PubMed: 19631565]
9. Choi YS, Kageyama R, Eto D, Escobar TC, Johnston RJ, Monticelli L, et al. ICOS receptor instructs T follicular helper cell versus effector cell differentiation via induction of the transcriptional repressor Bcl6. Immunity. 2011; 34(6):932–946. [PubMed: 21636296]
10. Kitano M, Moriyama S, Ando Y, Hikida M, Mori Y, Kurosaki T, et al. Bcl6 protein expression shapes pre-germinal center B cell dynamics and follicular helper T cell heterogeneity. Immunity. 2011; 34(6):961–972. [PubMed: 21636294]

11. Weinstein JS, Bertino SA, Hernandez SG, Poholek AC, Teplitzky TB, Nowyhed HN, et al. B cells in T follicular helper cell development and function: separable roles in delivery of ICOS ligand and antigen. J Immunol. 2014; 192(7):3166–3179. [PubMed: 24610013]
12. Yusuf I, Kageyama R, Monticelli L, Johnston RJ, DiToro D, Hansen K, et al. Germinal center T follicular helper cell IL-4 production is dependent on Signaling Lymphocytic Activation Molecule Receptor (CD150). J Immunol. 2010; 185(1):190–202. [PubMed: 20525889]
13. Sage PT, Francisco LM, Carman CV, Sharpe AH. The receptor PD-1 controls follicular regulatory T cells in the lymph nodes and blood. Nat Immunol. 2013; 14(2):152–161. [PubMed: 23242415]
14. Bossaller L, Burger J, Draeger R, Grimbacher B, Knoth R, Plebani A, et al. ICOS deficiency is associated with a severe reduction of CXCR5+CD4 germinal center Th cells. J Immunol. 2006; 177(7):4927–4932. [PubMed: 16982935]
15. Grimbacher B, Hutloff A, Schlesier M, Glocker E, Warnatz K, Drager R, et al. Homozygous loss of ICOS is associated with adult-onset common variable immunodeficiency. Nat Immunol. 2003; 4(3):261–268. [PubMed: 12577056]
16. Dong C, Juedes AE, Temann UA, Shresta S, Allison JP, Ruddle NH, et al. ICOS co-stimulatory receptor is essential for T-cell activation and function. Nature. 2001; 409(6816):97–101. [PubMed: 11343121]
17. McAdam AJ, Greenwald RJ, Levin MA, Chernova T, Malenkovich N, Ling V, et al. ICOS is critical for CD40-mediated antibody class switching. Nature. 2001; 409(6816):102–105. [PubMed: 11343122]
18. Tafuri A, Shahinian A, Bladt F, Yoshinaga SK, Jordana M, Wakeham A, et al. ICOS is essential for effective T-helper-cell responses. Nature. 2001; 409(6816):105–109. [PubMed: 11343123]
19. Mak TW, Shahinian A, Yoshinaga SK, Wakeham A, Boucher LM, Pintilie M, et al. Costimulation through the inducible costimulator ligand is essential for both T helper and B cell functions in T cell-dependent B cell responses. Nat Immunol. 2003; 4(8):765–772. [PubMed: 12833154]
20. Coyle AJ, Lehar S, Lloyd C, Tian J, Delaney T, Manning S, et al. The CD28-related molecule ICOS is required for effective T cell-dependent immune responses. Immunity. 2000; 13(1):95–105. [PubMed: 10933398]
21. Fos C, Salles A, Lang V, Carrette F, Audebert S, Pastor S, et al. ICOS ligation recruits the p50alpha PI3K regulatory subunit to the immunological synapse. J Immunol. 2008; 181(3):1969–1977. [PubMed: 18641334]
22. Kong KF, Fu G, Zhang Y, Yokosuka T, Casas J, Canonigo-Balancio AJ, et al. Protein kinase C-eta controls CTLA-4-mediated regulatory T cell function. Nat Immunol. 2014; 15(5):465–472. [PubMed: 24705298]
23. Kong KF, Yokosuka T, Canonigo-Balancio AJ, Isakov N, Saito T, Altman A. A motif in the V3 domain of the kinase PKC-theta determines its localization in the immunological synapse and functions in T cells via association with CD28. Nat Immunol. 2011; 12(11):1105–1112. [PubMed: 21964608]
24. Rudd CE, Schneider H. Unifying concepts in CD28, ICOS and CTLA4 co-receptor signalling. Nat Rev Immunol. 2003; 3(7):544–556. [PubMed: 12876557]
25. Gigoux M, Shang J, Pak Y, Xu M, Choe J, Mak TW, et al. Inducible costimulator promotes helper T-cell differentiation through phosphoinositide 3-kinase. Proc Natl Acad Sci U S A. 2009; 106(48):20371–20376. [PubMed: 19915142]
26. Li J, Heinrichs J, Leconte J, Haarberg K, Semple K, Liu C, et al. Phosphatidylinositol 3-kinase-independent signaling pathways contribute to ICOS-mediated T cell costimulation in acute graft-versus-host disease in mice. J Immunol. 2013; 191(1):200–207. [PubMed: 23729441]
27. Rolf J, Bell SE, Kovesdi D, Janas ML, Soond DR, Webb LM, et al. Phosphoinositide 3-kinase activity in T cells regulates the magnitude of the germinal center reaction. J Immunol. 2010; 185(7):4042–4052. [PubMed: 20826752]
28. Nance JP, Belanger S, Johnston RJ, Hu JK, Takemori T, Crotty S. Bcl6 middle domain repressor function is required for T follicular helper cell differentiation and utilizes the corepressor MTA3. Proc Natl Acad Sci U S A. 2015; 112(43):13324–13329. [PubMed: 26460037]
29. Akira S, Takeda K. Toll-like receptor signalling. Nat Rev Immunol. 2004; 4(7):499–511. [PubMed: 15229469]

30. Goenka R, Barnett LG, Silver JS, O'Neill PJ, Hunter CA, Cancro MP, et al. Cutting edge: dendritic cell-restricted antigen presentation initiates the follicular helper T cell program but cannot complete ultimate effector differentiation. J Immunol. 2011; 187(3):1091–1095. [PubMed: 21715693]

31. Barnett LG, Simkins HMA, Barnett BE, Korn LL, Johnson AL, Wherry EJ, et al. B cell antigen presentation in the initiation of follicular helper T cell and germinal center differentiation. J Immunol. 2014; 192(8):3607–3617. [PubMed: 24646739]

32. Tubo NJ, Pagan AJ, Taylor JJ, Nelson RW, Linehan JL, Ertelt JM, et al. Single naive CD4+ T cells from a diverse repertoire produce different effector cell types during infection. Cell. 2013; 153(4): 785–796. [PubMed: 23663778]

33. Häcker H, Redecke V, Blagoev B, Kratchmarova I, Hsu LC, Wang GG, et al. Specificity in Toll-like receptor signalling through distinct effector functions of TRAF3 and TRAF6. Nature. 2006; 439(7073):204–207. [PubMed: 16306937]

34. Sato S, Sugiyama M, Yamamoto M, Watanabe Y, Kawai T, Takeda K, et al. Toll/IL-1 Receptor Domain-Containing Adaptor Inducing IFN-β (TRIF) Associates with TNF Receptor-Associated Factor 6 and TANK-Binding Kinase 1, and Activates Two Distinct Transcription Factors, NF-κB and IFN-Regulatory Factor-3, in the Toll-Like Receptor Signaling. J Immunol. 2003; 171(8):4304–4310. [PubMed: 14530355]

35. Sharma S, tenOever BR, Grandvaux N, Zhou GP, Lin R, Hiscott J. Triggering the interferon antiviral response through an IKK-related pathway. Science. 2003; 300(5622):1148–1151. [PubMed: 12702806]

36. Fitzgerald KA, McWhirter SM, Faia KL, Rowe DC, Latz E, Golenbock DT, et al. IKKepsilon and TBK1 are essential components of the IRF3 signaling pathway. Nat Immunol. 2003; 4(5):491–496. [PubMed: 12692549]

37. McWhirter SM, Pullen SS, Holton JM, Crute JJ, Kehry MR, Alber T. Crystallographic analysis of CD40 recognition and signaling by human TRAF2. Proc Natl Acad Sci U S A. 1999; 96(15): 8408–8413. [PubMed: 10411888]

38. Bonnard M, Mirtsos C, Suzuki S, Graham K, Huang J, Ng M, et al. Deficiency of T2K leads to apoptotic liver degeneration and impaired NF-kappaB-dependent gene transcription. EMBO J. 2000; 19(18):4976–4985. [PubMed: 10990461]

39. Jin J, Xiao Y, Chang JH, Yu J, Hu H, Starr R, et al. The kinase TBK1 controls IgA class switching by negatively regulating noncanonical NF-kappaB signaling. Nat Immunol. 2012; 13(11):1101–1109. [PubMed: 23023393]

40. Ishii KJ, Kawagoe T, Koyama S, Matsui K, Kumar H, Kawai T, et al. TANK-binding kinase-1 delineates innate and adaptive immune responses to DNA vaccines. Nature. 2008; 451(7179):725–729. [PubMed: 18256672]

41. Pomerantz JL, Baltimore D. NF-kappaB activation by a signaling complex containing TRAF2, TANK and TBK1, a novel IKK-related kinase. EMBO J. 1999; 18(23):6694–6704. [PubMed: 10581243]

42. Oganesyan G, Saha SK, Guo B, He JQ, Shahangian A, Zarnegar B, et al. Critical role of TRAF3 in the Toll-like receptor-dependent and -independent antiviral response. Nature. 2006; 439(7073): 208–211. [PubMed: 16306936]

43. Li C, Norris PS, Ni CZ, Havert ML, Chiong EM, Tran BR, et al. Structurally Distinct Recognition Motifs in Lymphotoxin-β Receptor and CD40 for Tumor Necrosis Factor Receptor-associated Factor (TRAF)-mediated Signaling. J Biol Chem. 2003; 278(50):50523–50529. [PubMed: 14517219]

44. Linterman MA, Rigby RJ, Wong R, Silva D, Withers D, Anderson G, et al. Roquin differentiates the specialized functions of duplicated T cell costimulatory receptor genes CD28 and ICOS. Immunity. 2009; 30(2):228–241. [PubMed: 19217324]

45. Linterman MA, Denton AE, Divekar DP, Zvetkova I, Kane L, Ferreira C, et al. CD28 expression is required after T cell priming for helper T cell responses and protective immunity to infection. Elife. 2014; 3

46. Weber JP, Fuhrmann F, Feist RK, Lahmann A, Al Baz MS, Gentz LJ, et al. ICOS maintains the T follicular helper cell phenotype by down-regulating Kruppel-like factor 2. J Exp Med. 2015; 212(2):217–233. [PubMed: 25646266]

47. Leavenworth JW, Verbinnen B, Yin J, Huang H, Cantor H. A p85alpha-osteopontin axis couples the receptor ICOS to sustained Bcl-6 expression by follicular helper and regulatory T cells. Nat Immunol. 2015; 16(1):96–106. [PubMed: 25436971]

48. Nurieva RI, Chung Y, Hwang D, Yang XO, Kang HS, Ma L, et al. Generation of T follicular helper cells is mediated by interleukin-21 but independent of T helper 1, 2, or 17 cell lineages. Immunity. 2008; 29(1):138–149. [PubMed: 18599325]

49. Xu H, Li X, Liu D, Li J, Zhang X, Chen X, et al. Follicular T-helper cell recruitment governed by bystander B cells and ICOS-driven motility. Nature. 2013; 496(7446):523–527. [PubMed: 23619696]

Methods-only References

50. Sanjo H, Zajonc DM, Braden R, Norris PS, Ware CF. Allosteric Regulation of the Ubiquitin:NIK and Ubiquitin:TRAF3 E3 Ligases by the Lymphotoxin-β Receptor. J Biol Chem. 2010; 285(22): 17148–17155. [PubMed: 20348096]

51. Chen R, Belanger S, Frederick MA, Li B, Johnston RJ, Xiao N, et al. In vivo RNA interference screens identify regulators of antiviral CD4(+) and CD8(+) T cell differentiation. Immunity. 2014; 41(2):325–338. [PubMed: 25148027]

52. Washburn MP, Wolters D, Yates JR 3rd. Large-scale analysis of the yeast proteome by multidimensional protein identification technology. Nat Biotechnol. 2001; 19(3):242–247. [PubMed: 11231557]

53. Xu T, Venable JD, Park SK, Cociorva D, Lu B, Liao L, et al. ProLuCID, a fast and sensitive tandem mass spectra-based protein identification program. Mol Cell Proteomics. 2006; 5(10):S174–S174.

54. Tabb DL, McDonald WH, Yates JR. DTASelect and contrast: Tools for assembling and comparing protein identifications from shotgun proteomics. J Proteome Res. 2002; 1(1):21–26. [PubMed: 12643522]

55. Park SK, Venable JD, Xu T, Yates JR. A quantitative analysis software tool for mass spectrometry-based proteomics. Nat Methods. 2008; 5(4):319–322. [PubMed: 18345006]

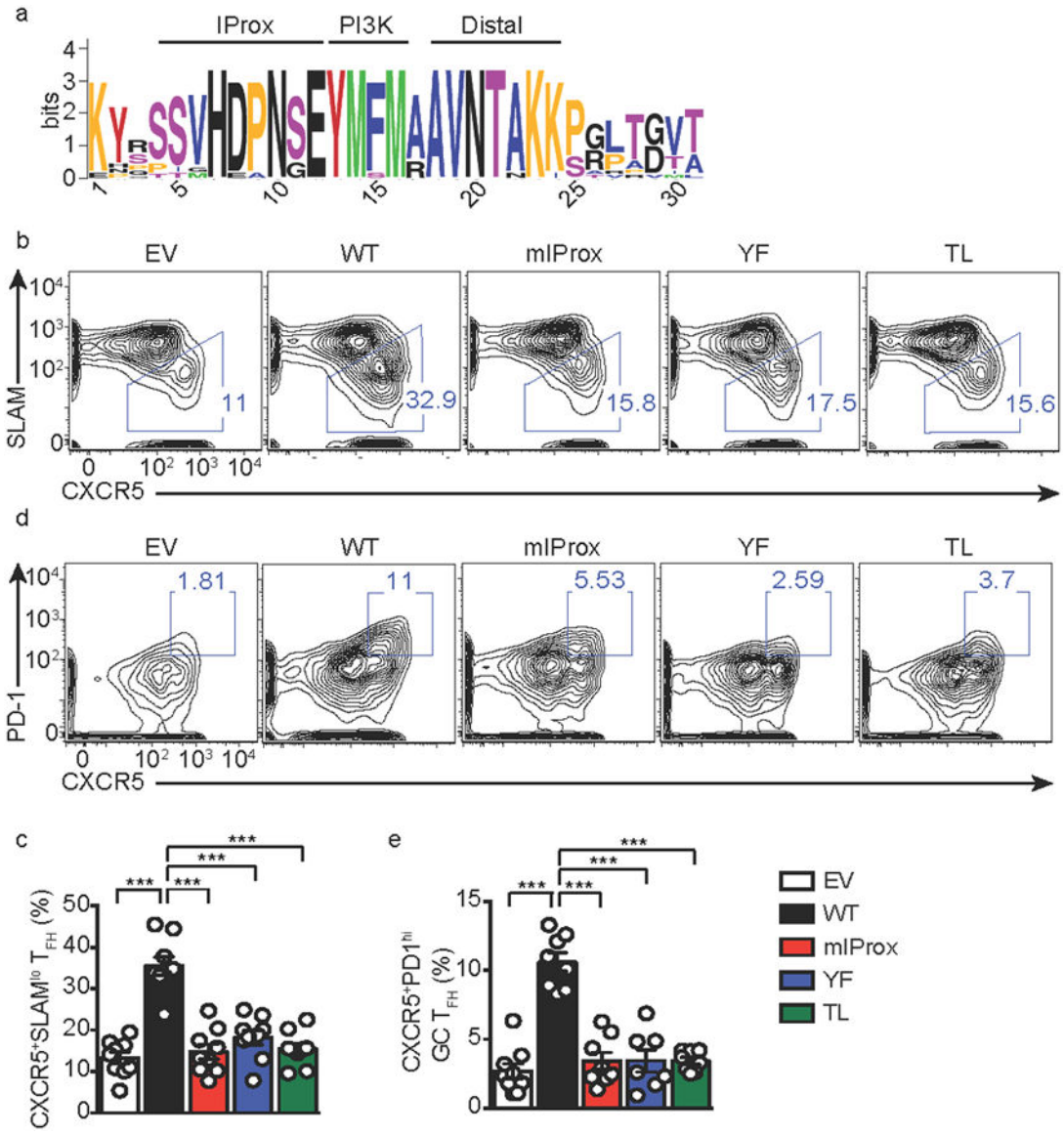

Figure 1a

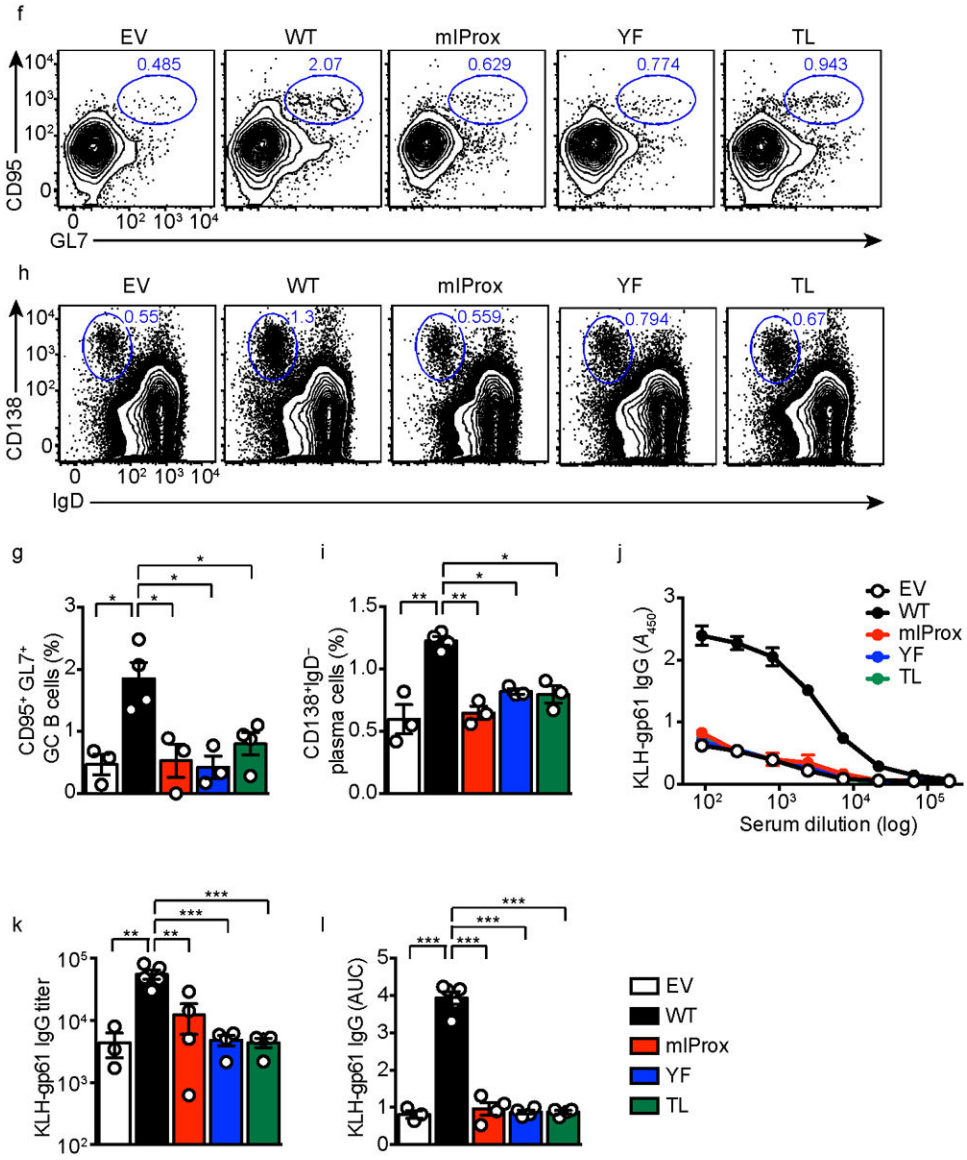

Figure 1b

Figure 1.

Importance of a novel ICOS signaling motif in T_{FH} cell development. (**a**) Evolutionary conservation of the proximal (IProx), PI3K-binding YxxM and distal motifs in the cytoplasmic tail of ICOS. (**b**,**d**) Flow cytometry of cells from host B6 mice 7 d after adoptive transfer of *Icos*$^{-/-}$ SMARTA CD4^{+} T cells transduced with retrovirus encoding empty vector (EV) or wild-type ICOS (WT) or mIProx, YF or TL mutant ICOS and infected with LCMV Armstrong strain. Numbers adjacent to outlined areas indicate percent CXCR5^{+}SLAM^{lo} T_{FH} cells (**b**) or CXCR5^{+}PD1^{hi} GC T_{FH} cells (**d**). Cumulative data for **b** (**c**) or **d** (**e**) from three independent experiments. (**f**, **h**) Flow cytometry of cells from host CD4-Cre × *Bcl6*$^{fl/fl}$ mice 10 d after adoptive transfer of *Icos*$^{-/-}$ SMARTA CD4^{+} T cells transduced as in (**b**), and were immunized with KLH-gp61 absorbed to alum. Numbers adjacent to outlined areas indicate percent CD95^{+}GL7^{+} GC B cells (**f**) and CD138^{+}IgD^{-} plasma cells (**h**). Cumulative

data for **f** (**g**) or **h** (**i**) from two independent experiments. Each data point represents a single mouse. (**j**) Quantification of anti-KLH-gp61 IgG from sera of immunized mice analyzed with ELISA and presented as absorbance at 450 nm. The endpoint titer (**k**) and area under curve (AUC; **l**) were calculated. Shown are mean ± SEM; ANOVA with *post-hoc* Tukey's corrections. $*P < 0.01$; $**P < 0.001$; $***P < 0.0001$.

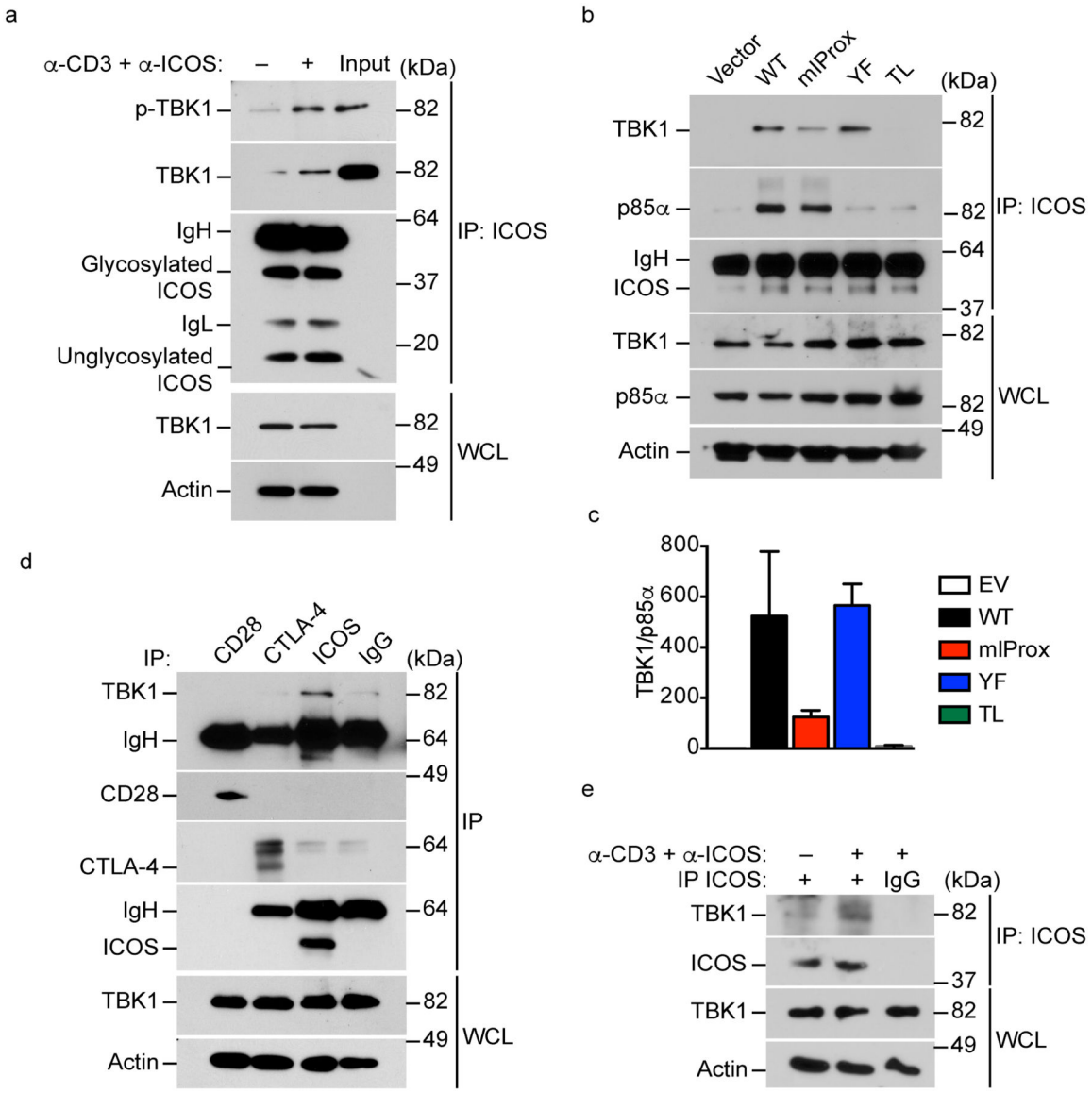

Figure 2.

ICOS-TBK1 interaction. (**a**) ICOS immunoprecipitations (IPs) from mouse primary $CD4^+$ T cells activated *in vitro* with anti-CD3 plus anti-CD28 and rested in IL-2, followed by restimulation with anti-CD3 plus anti-ICOS. IPs or whole cell lysates (WCL) were immunoblotted with the indicated Abs. 5 % WCL was used as input to control for immunoprecipitation. (**b**) ICOS IPs of Jurkat T cells transfected with WT, mIProx, YF or tailless (TL) mutants stimulated with anti-CD3 plus anti-ICOS. Intensity of TBK1 and p85α bands was quantified using ImageJ software and expressed as ratio of TBK1:p85α (**c**). Shown are mean ± SEM. $p > 0.05$ for comparative analyses of all groups; ANOVA with *post-hoc* Tukey's corrections. (**d**) IPs of *in vitro* activated primary mouse $CD4^+$ T cells stimulated with anti-CD3 plus the indicated costimulatory Abs, and IP with the indicated costimulatory Abs. (**e**) ICOS IPs from human GC T_{FH} cells left unstimulated or stimulated

with anti-CD3 plus anti-ICOS. IPs or whole cell lysates (WCL) were immunoblotted with the indicated Abs. All IP data are representative of three experiments.

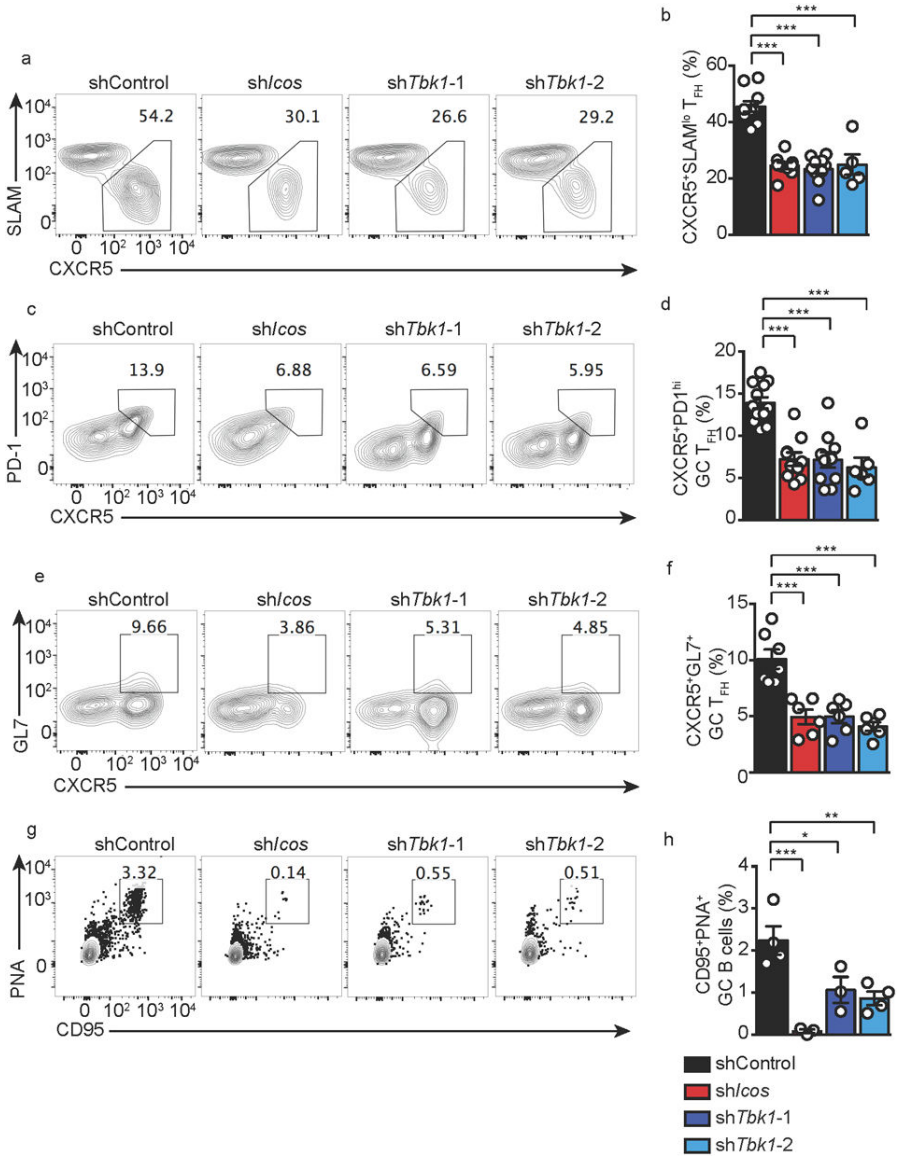

Figure 3a

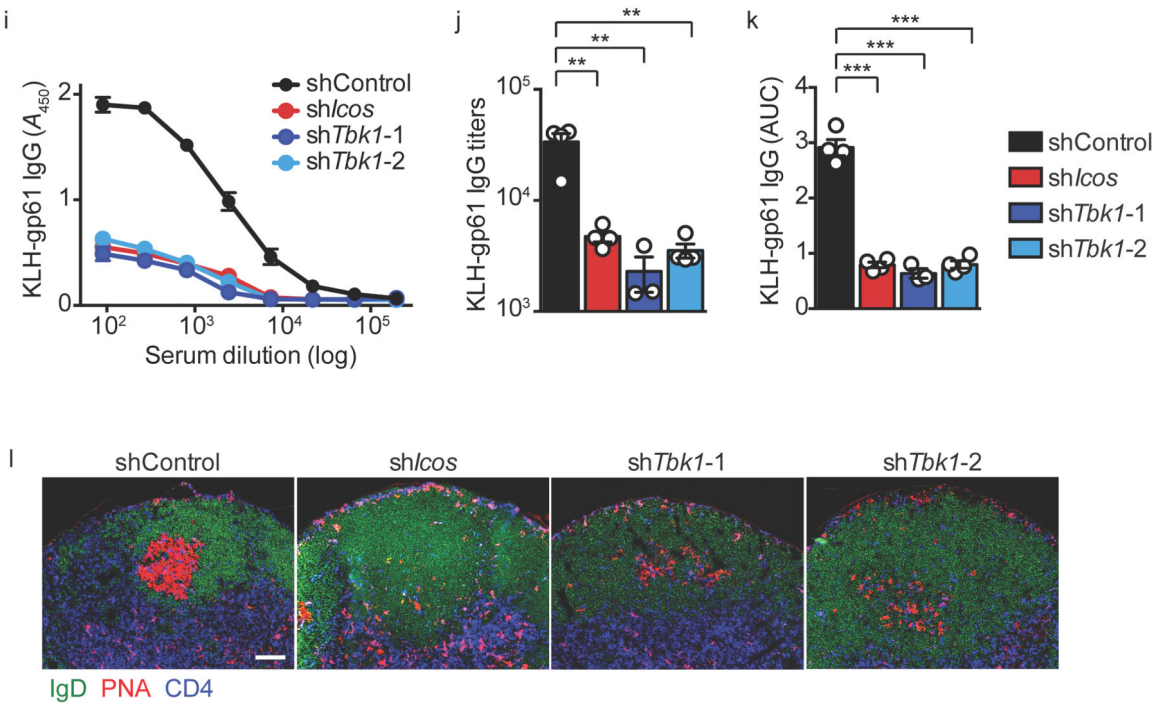

Figure 3b

Figure 3.

TBK1 is required for T_{FH} cell differentiation. (**a**, **c**, **e**) Flow cytometry of cells from host B6 mice 7 d after adoptive transfer of SMARTA $CD4^+$ T cells transduced with shRNA targeting the *Tbk1* (sh*Tbk1*-1 and sh*Tbk1*-2), *Icos* or control genes and infected with LCMV Armstrong strain. Numbers adjacent to outlined areas indicate percent $CXCR5^+SLAM^{lo}$ T_{FH} cells (**a**), $CXCR5^+PD1^{hi}$ GC T_{FH} cells (**c**), or $CXCR5^+GL7^{hi}$ GC T_{FH} cells (**e**). Cumulative data for **a** (**b**), **c** (**d**) or **e** (**f**) from three independent experiments. (**g**) Flow cytometry of cells from host CD4-Cre × $Bcl6^{fl/fl}$ mice 10 d after adoptive transfer of $Icos^{-/-}$ SMARTA $CD4^+$ T cells transduced as in (**a**), and were immunized with KLH-gp61 suspended in AddaVax. Numbers adjacent to outlined areas indicate percent $CD95^+PNA^+$ GC B cells. Cumulative data for **g** (**h**) from two independent experiments. (**i**) Quantification of anti-KLH-gp61 IgG from sera of immunized mice analyzed with ELISA and presented as absorbance at 450 nm. The endpoint titer (**j**) and area under curve (AUC; **k**) were calculated. Each data point represents a single mouse. Shown are mean ± SEM; ANOVA with *post-hoc* Tukey's corrections. $*P < 0.01$; $**P < 0.001$; $***P < 0.0001$. (**l**) Immunofluorescence staining of LN showing PNA^+ germinal centers from host CD4-Cre × $Bcl6^{fl/fl}$ mice 10 d after adoptive transfer of $Icos^{-/-}$ SMARTA $CD4^+$ T cells transduced as in (**a**). Scale bar, 100 μm; 20× magnification.

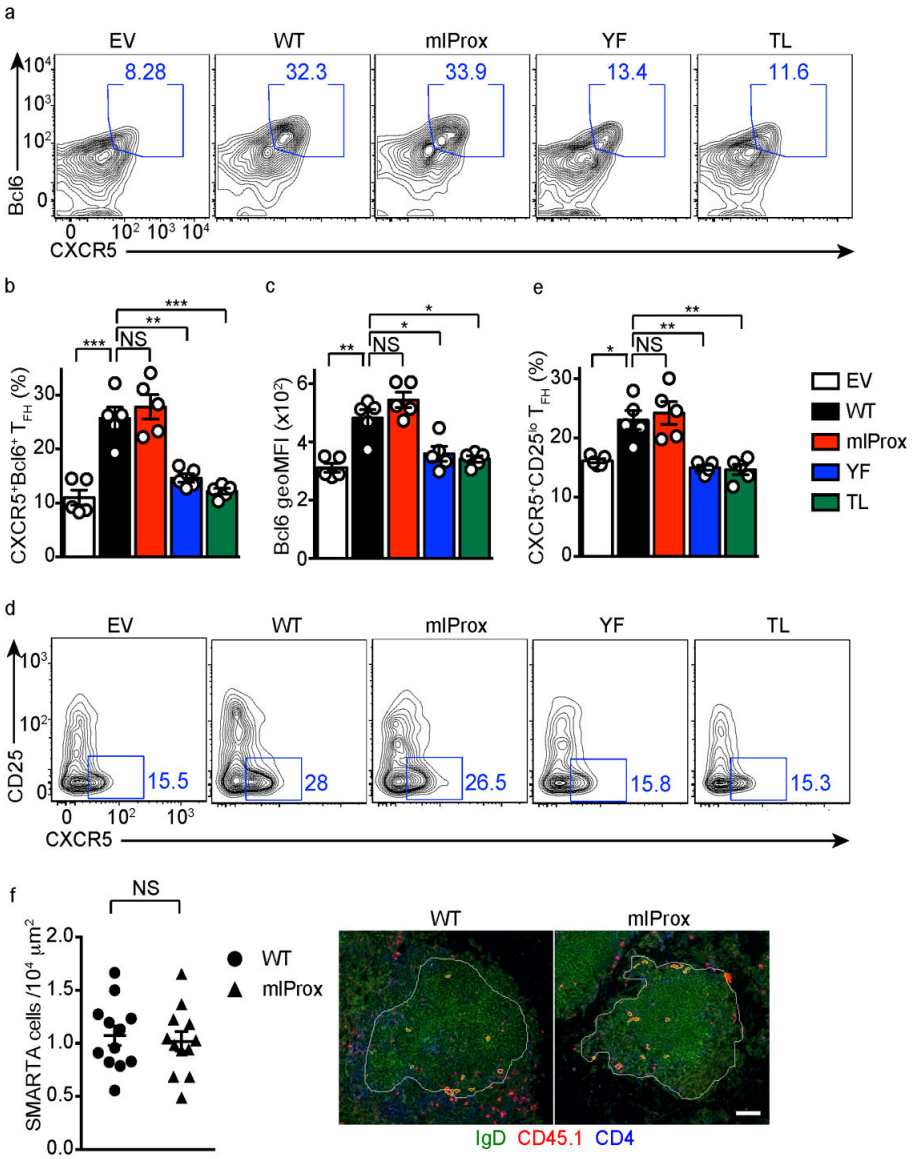

Figure 4.

The IProx ICOS motif is dispensable for nascent T_{FH} cell development. (**a**, **d**) Flow cytometry of cells from host B6 mice 3 d after adoptive transfer of *Icos*$^{-/-}$ SMARTA CD4^{+} T cells transduced with RV encoding empty vector (EV), WT, mIProx, YF or TL and infected with LCMV Armstrong strain. Numbers adjacent to outlined areas indicate percent Bcl6^{+}CXCR5^{+} (**a**) or CXCR5^{+}CD25^{lo} T_{FH} cells (**d**). Cumulative data for **a** (**b**) or **d** (**e**) from two independent experiments. (**c**) Mean fluorescent intensity of Bcl6 protein in CD4^{+}GFP^{+} T cells. Each data point represents a single mouse. Shown are mean ± SEM. *$P < 0.01$; **$P < 0.001$; ***$P < 0.0001$; NS: not significant; ANOVA with *post-hoc* Tukey's corrections. (**f**) Quantification of CD45.1^{+} cells in B-cell follicles from host B6 mice 4 d after adoptive transfer of congenic CD45.1^{+} *Icos*$^{-/-}$ SMARTA CD4^{+} T cells reconstituted with WT or mIProx and infected with LCMV Armstrong strain. CD45.1^{+} T cells found in B-cell follicles and at the T:B border were enumerated and normalized to the area. Each data point

represents a B cell follicle. Shown are representative immunofluorescence images outlining B-cell follicles and the identified CD45.1^{+} T cells transduced with WT or mIProx. Scale bar, 100 μm; 20× magnification. Graph is mean ± SEM; NS: not significant; Mann-Whitney U test.

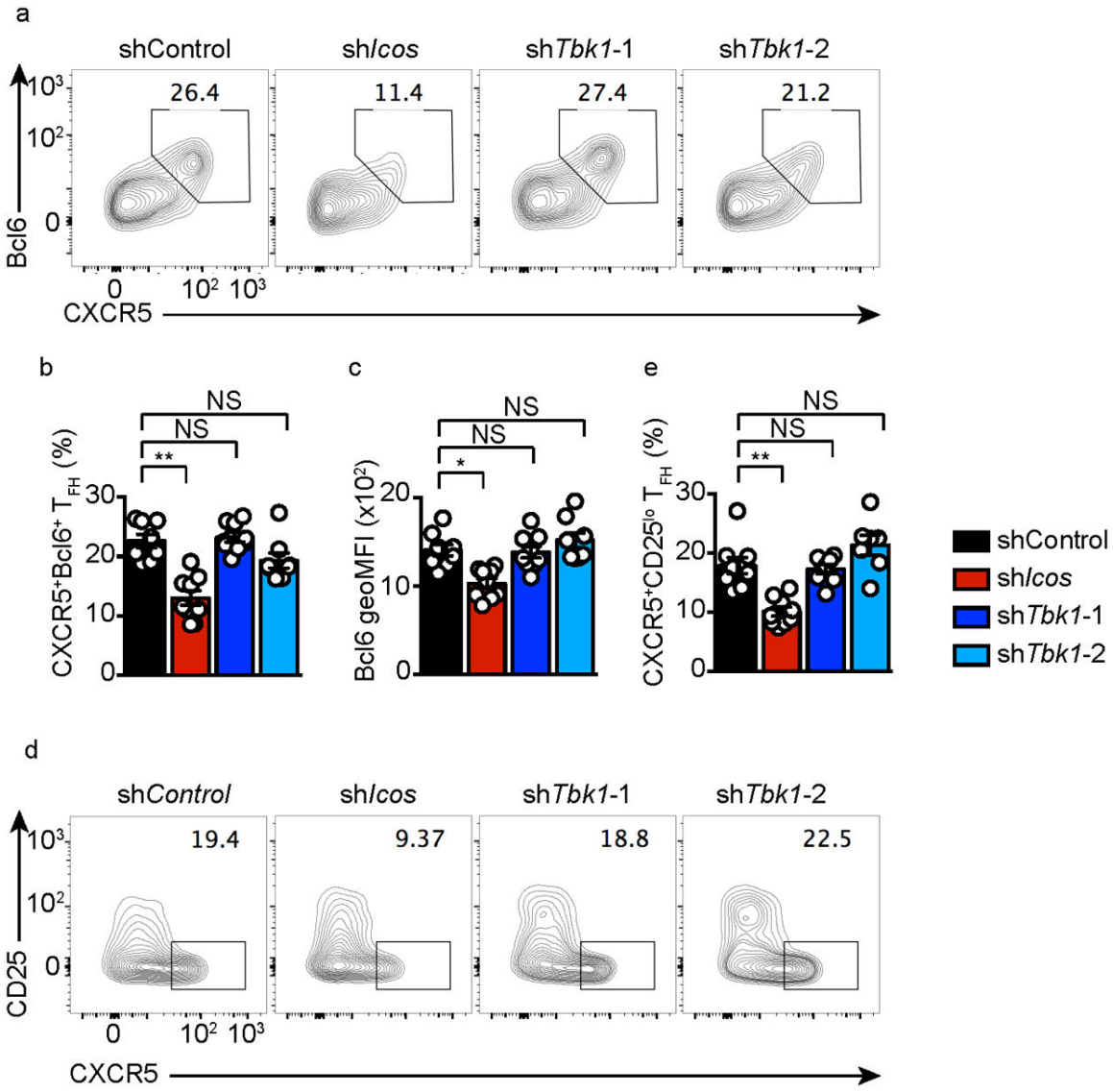

Figure 5.

TBK1 is dispensable for nascent T_{FH} differentiation. (**a**, **d**) Flow cytometry of cells from host B6 mice 3 d after adoptive transfer of SMARTA $CD4^+$ T cells transduced with shRNA targeting the *Tbk1* (sh*Tbk1*-1 and sh*Tbk1*-2), *Icos* or control genes and infected with LCMV Armstrong strain. Numbers adjacent to outlined areas indicate percent $CXCR5^+Bcl6^+$ (**a**) or $CXCR5^+CD25^{lo}$ T_{FH} cells (**d**). Cumulative data for **a** (**b**) or **d** (**e**) from two independent experiments. (**c**) Mean fluorescent intensity of Bcl6 protein expression in $CD4^+GFP^+$ T cells. Each data point represents a single mouse. Shown are mean ± SEM. $*P < 0.01$; $**P < 0.001$; $***P < 0.0001$; NS: not significant; ANOVA with *post-hoc* Tukey's corrections.

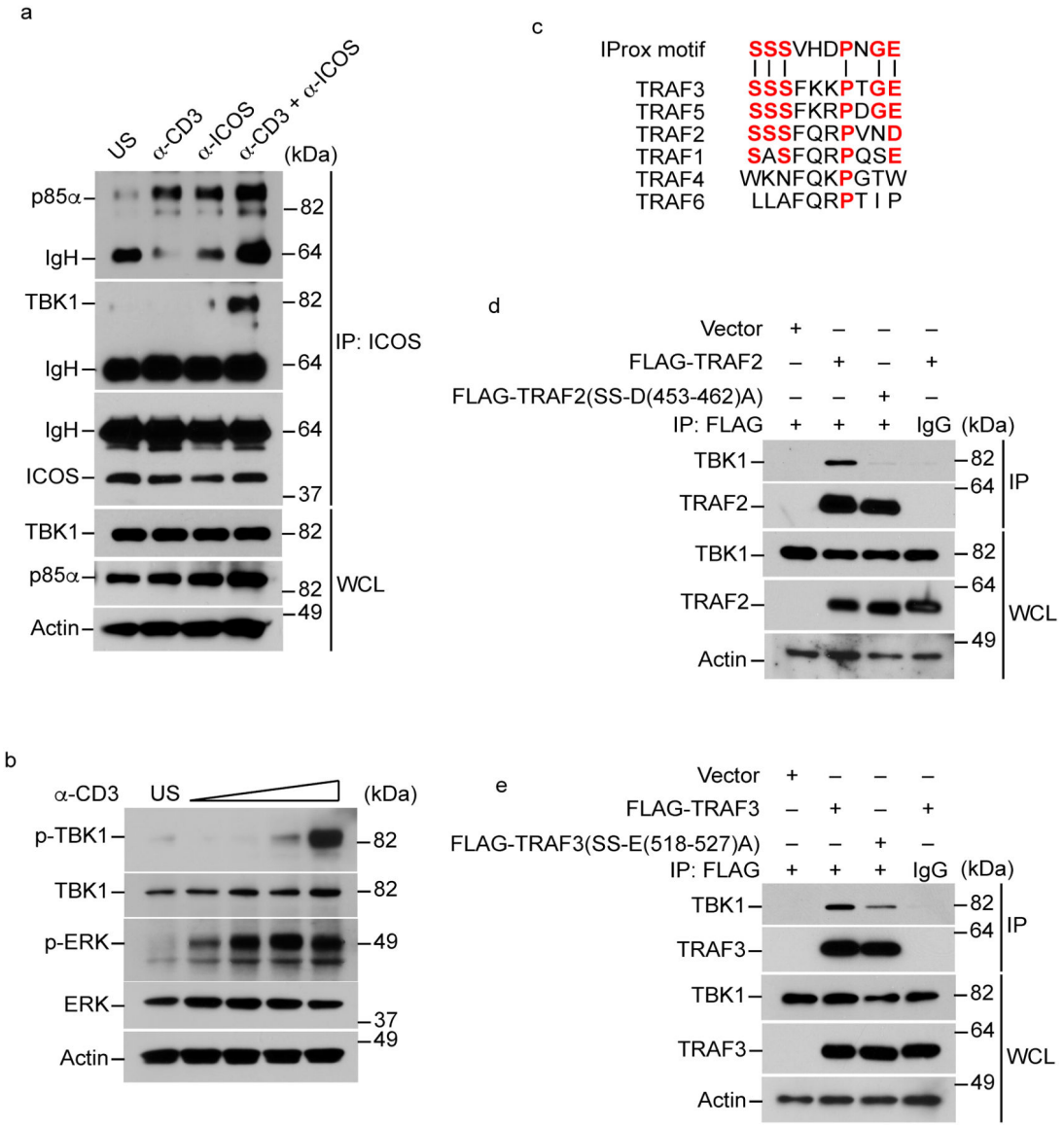

Figure 6.

Molecular basis of ICOS-TBK1 interaction. (**a**) ICOS IPs from *in vitro* activated primary mouse $CD4^+$ T cells left unstimulated (US) or stimulated with cross-linked anti-CD3 alone, anti-ICOS alone, or a combination of both Abs. IPs or WCL were immunoblotted with the indicated Abs. (**b**) Blotting of *in vitro* activated primary mouse $CD4^+$ T cells left unstimulated (US) or stimulated with increasing concentration of anti-CD3 mAb (10^{-2}, 10^{-1}, 10^0 and 10^1 μg/ml) plus anti-ICOS (5 μg/ml). WCL were immunoblotted with the indicated Abs. ERK phosphorylation (p-ERK) was used as a surrogate marker for T cell activation. (**c**) Alignment of the motif shared between the IProx motif and TRAF proteins. (**d**, **e**) TRAF IPs from human HEK293T cells transfected with FLAG-tagged WT or mutated TRAF2 (**d**) or TRAF3 (**e**). Anti-FLAG IPs or WCL were immunoblotted with the indicated Abs. All data are representative of three experiments.

Table 1

List of cytosolic proteins identified through SILAC analyses. Jurkat T cells transfected with WT or mIProx were metabolically labeled and analyzed using mass spectrometry following stimulation with anti-CD3 plus anti-ICOS, and anti-ICOS IP. Shown are proteins with >4 identifying peptides with significant difference ($P < 0.05$) and > 1.5 fold-change between WT and mIProx.

Protein	Putative Function	Fold change
TBK1	Signaling kinase	7.69
MYCBP2	E3 ligase	5.26
BAG6	Chaperone	3.13
NAA10	Acetyltransferase	2.95
GAK	Cell cycle kinase	2.17
SLP76	TCR signaling adaptor	2.08
Erlin2	ER protein	1.81
GSTZ1	Metabolism	1.64
KLC1	Cytoskeleton	1.59